

OPEN ACCESS

EDITED BY

Mahmood Sadat-Noori,
University of New South Wales, Australia

REVIEWED BY

Chunyu Zhao,
Dezhou University, China
Sairah Malkin,
University of Maryland, College Park,
United States

*CORRESPONDENCE

Dunia Rios-Yunes

✉ unia.rios.yunes@nioz.nl

SPECIALTY SECTION

This article was submitted to
Marine Biogeochemistry,
a section of the journal
Frontiers in Marine Science

RECEIVED 31 January 2023

ACCEPTED 10 March 2023

PUBLISHED 22 March 2023

CITATION

Rios-Yunes D, Grandjean T, di Primio A,
Tiano J, Bouma TJ, van Oevelen D and
Soetaert K (2023) Sediment
resuspension enhances nutrient
exchange in intertidal mudflats.
Front. Mar. Sci. 10:1155386.
doi: 10.3389/fmars.2023.1155386

COPYRIGHT

© 2023 Rios-Yunes, Grandjean, di Primio,
Tiano, Bouma, van Oevelen and Soetaert.
This is an open-access article distributed
under the terms of the [Creative Commons
Attribution License \(CC BY\)](https://creativecommons.org/licenses/by/4.0/). The use,
distribution or reproduction in other
forums is permitted, provided the original
author(s) and the copyright owner(s) are
credited and that the original publication in
this journal is cited, in accordance with
accepted academic practice. No use,
distribution or reproduction is permitted
which does not comply with these terms.

Sediment resuspension enhances nutrient exchange in intertidal mudflats

Dunia Rios-Yunes^{1*}, Tim Grandjean^{1,2}, Alena di Primio³,
Justin Tiano⁴, Tjeerd J. Bouma^{1,2}, Dick van Oevelen¹
and Karline Soetaert¹

¹Department of Estuarine and Delta Systems, Royal Netherlands Institute for Sea Research (NIOZ), Yerseke, Netherlands, ²Faculty of Geosciences, Department of Physical Geography, Utrecht University, Utrecht, Netherlands, ³Department of microbiology and biogeochemistry, Royal Netherlands Institute for Sea Research (NIOZ), Den Burg, Netherlands, ⁴Wageningen Marine Research, Wageningen University and Research, IJmuiden, Netherlands

Intertidal coastal sediments are important centers for nutrient transformation, regeneration, and storage. Sediment resuspension, due to wave action or tidal currents, can induce nutrient release to the water column and fuel primary production. Storms and extreme weather events are expected to increase due to climate change in coastal areas, but little is known about their effect on nutrient release from coastal sediments. We have conducted *in-situ* sediment resuspension experiments, in which erosion was simulated by a stepwise increase in current velocities, while measuring nutrient uptake or release in field flumes positioned on intertidal areas of a tidal bay (Eastern Scheldt) and an estuary (Western Scheldt). In both systems, the water column concentration of ammonium (NH_4^+) and nitrite (NO_2^-) increased predictably with greater erosion as estimated from pore water dilution and erosion depth. In contrast, the phosphate (PO_4^{3-}) dynamics were different between systems, and those of nitrate (NO_3^-) were small and variable. Notably, sediment resuspension caused a decrease in the overlying water PO_4^{3-} concentration in the tidal bay, while an increase was observed in the estuarine sediments. Our observations showed that the concentration of PO_4^{3-} in the water column was more intensely affected by resuspension than that of NH_4^+ and NO_2^- . The present study highlights the differential effect of sediment resuspension on nutrient exchange in two contrasting tidal coastal environments.

KEYWORDS

intertidal sediments, nutrient release, biogeochemistry, sediment resuspension, coastal erosion, eutrophication

1 Introduction

Intertidal sediments are centers of organic matter (OM) remineralization, nutrient recycling, transformation, and removal (Boynton et al., 2018; Lessin et al., 2018; Rios-Yunes et al., 2023a). Solute exchange between sediments and the water column is crucial for the functioning of coastal ecosystems as it affects the concentration of nutrients available

for primary production. This exchange is generally caused by passive diffusion, bioturbation and bioirrigation (Aller, 1982; Braeckman et al., 2010; De Borger et al., 2020), or sediment resuspension from wave and tidal action (Cabrita et al., 1999; Tengberg et al., 2003; Kalnejais et al., 2010). It can also be triggered by human activities such as dredging and bottom trawling (Morin and Morse, 1999; Dounas et al., 2007; Tiano et al., 2021).

Sediment resuspension and coastal erosion are expected to increase due to climate change-related alterations of wind patterns as well as the magnitude and frequency of extreme weather events such as storms and hurricanes (Woth et al., 2006; Statham, 2012; Chen et al., 2018; Niemistö and Lund-Hansen, 2019). During a resuspension event, nutrients and dissolved OM in the water column can adsorb onto resuspended sediment particles and decrease their concentration in the water column (Tengberg et al., 2003; Tiano et al., 2019). Alternatively, pore water nutrients, whose concentration in the sediment is typically higher than in the water column, may be released into the overlying water at the equivalent of several days of undisturbed fluxes (sum of diffusive and fauna-induced fluxes) (Tiano et al., 2021). An erosion event can also release OM previously stored in sediments resulting in an increase in bacterial mineralization in the water column and higher utilization of dissolved oxygen (DO) (Tengberg et al., 2003).

Enhanced nutrient concentrations in the water column (Tengberg et al., 2003; Kalnejais et al., 2010; Niemistö and Lund-Hansen, 2019) have been observed to harm coastal ecosystems worldwide (Malone and Newton, 2020). The list of detrimental effects includes harmful algal blooms, eutrophication, habitat loss, the disappearance of macrobenthic communities, coastal acidification, deoxygenation, and dead zones (Qin et al., 2004; Breitburg et al., 2018; Chen et al., 2018; Malone and Newton, 2020). Indeed, studies in lacustrine environments have reported eutrophic conditions and algal blooms following resuspension events (Ogilvie and Mitchell, 1998; Qin et al., 2004; Schallenberg and Burns, 2004; Dzialowski et al., 2008). Understanding how sediment resuspension affects nutrient release is important given the current worldwide challenges associated with nutrient dynamics and enrichment in coastal areas (Malone and Newton, 2020). This knowledge could aid eutrophication management efforts by identifying sediments which are sensitive to disturbance-induced nutrient release or areas important for nutrient storage. In addition, it could help identify areas whose nutrient storage capacity could be compromised by increased storm frequency.

Shallow marine sediments and estuaries may be expected to react similarly to resuspension, however, relatively few studies have been conducted on the topic, and those that did, yielded inconsistent results (Morin and Morse, 1999; Chen et al., 2018; Niemistö and Lund-Hansen, 2019). Local abiotic conditions like salinity, grain size and the concentration and origin of OM in the sediment play an important role in determining the type of biogeochemical reactions occurring in coastal areas (Jordan et al., 2008; Loucaide et al., 2008; Rios-Yunes et al., 2023a). For example, phosphate sorption-desorption depends on salinity, but also on the concentration of DSi (Caraco et al., 1990; Jordan et al., 2008). Similarly, the concentration of OM and pore water nutrients is

closely associated with smaller grain sizes (Precht et al., 2004). Therefore, the combination of these parameters may determine the extent of nutrient release in coastal sediments.

We measured nutrient exchange between the sediment and water column following experimentally induced erosion in intertidal sediments from the Western Scheldt estuary (WS) and the Eastern Scheldt (ES) tidal bay, The Netherlands. After extensive engineering, the ES became a tidal bay, while the WS remained an estuary (Smaal and Nienhuis, 1992). The Western Scheldt and Eastern Scheldt are therefore a good case study because they display contrasting biogeochemical characteristics and sediment dynamics despite sharing a similar geological origin (Smaal and Nienhuis, 1992; Jiang et al., 2019; Rios-Yunes et al., 2023a; Rios-Yunes et al., 2023b). The aim of our study was to quantify instantaneous changes in nutrient concentration by causing sediment resuspension *in-situ*, and to determine its effects in the water column properties of two contrasting ecosystems: an estuary, and a tidal bay. We investigated sites along gradients of inundation time (high tidal zone and low tidal zone), salinity and grain size to define the biogeochemical differences amongst these systems and whether these differences influenced nutrient release due to erosion.

2 Materials and methods

2.1 Study sites

2.1.1 Eastern Scheldt tidal bay

The Eastern Scheldt tidal bay is a former estuary in the southwest of The Netherlands (Figure 1). The ES has a storm surge barrier, constructed in 1986, that isolates it from tidal exchange with the North Sea only during severe storm conditions. River inflow into the Eastern Scheldt is controlled by multiple sluices resulting in a negligible input of freshwater and sediments ($4.3 \text{ m}^3 \text{ s}^{-1}$) and nearly constant salinity ($S = 30$) (Jiang et al., 2019). Currently, the Eastern Scheldt is a flush-dominated system ($\sim 2 \times 10^4 \text{ m}^3 \text{ s}^{-1}$ tidal exchange over a 12 h tidal cycle) with a decreasing gradient of chlorophyll *a* (chl *a*), nutrient concentrations, suspended sediment, and turbidity from the North Sea in the west to the eastern section (Smaal and Nienhuis, 1992; Wetsteyn and Kromkamp, 1994; Jiang et al., 2019). The construction of the storm surge barrier and sluices triggered several alterations that ranged from geomorphological including the transformation from an estuary to a tidal bay, reduced sediment input, sand starvation, and constant erosion of intertidal areas (Smaal and Nienhuis, 1992; Nienhuis and Smaal, 1994; ten Brinke, 1994); to biological following the change of benthic species into a fully marine community (Ysebaert et al., 2016); and biogeochemical comprising the loss of the salinity gradient and decreased nutrient concentrations (Wetsteyn and Kromkamp, 1994).

2.1.2 Western Scheldt estuary

The Western Scheldt is a typical funnel-shaped estuary with a longitudinal salinity gradient. The Scheldt River starts in France, runs through Belgium, and ends in The Netherlands. At the Dutch



FIGURE 1

Map of sampling locations indicated with red diamonds. In the Western Scheldt: Appels (AP) in the freshwater, Groot Buitenschoor (GBS) and Rilland (RL) in the brackish, and Zuidgors (ZG) and Paulinapolder (PP) in the marine part. In the Eastern Scheldt: Rattekaai (RK), Dortsman (DT) and Zandkreek (ZK). Coordinates are in [Appendix 1](#).

– Belgian border, the Scheldt River becomes wider and mixes with the saline water from the North Sea creating a brackish zone, to finally discharge into the North Sea (Soetaert et al., 1994) (Figure 1). The salinity gradient in the brackish region is influenced by seasonal fluctuations in precipitation and riverine discharge (Baeyens et al., 1997; Struyf et al., 2004; Soetaert et al., 2006). The Western Scheldt used to be a eutrophic system with water column anoxia, but the implementation of water quality policies since 1970's has improved the water quality (Soetaert et al., 2006; Rios-Yunes et al., 2023a).

2.2 Sampling sites

Eight intertidal mudflats were sampled (Figure 1), three in the Eastern Scheldt: Dortsman (DT), Rattekaai (RK) and Zandkreek (ZK), and five along the salinity gradient of the Western Scheldt: Appels (AP), Groot Buitenschoor (GBS), Rilland (RL), Zuidgors (ZG) and Paulinapolder (PP). At each site, two locations were selected at 25 m (referred to as 'high tidal zone') and 200 m (referred to as 'low tidal zone') from the salt marsh edge, except for the narrow mudflats of Zandkreek (Eastern Scheldt) and Appels (Western Scheldt) where sampling was only done in the high tidal zone (Appendix 1). The sites exhibited a range of porosity and median grain sizes from muddy ($D_{50} 24.9 \pm 2.8 \mu\text{m}$) to sandy ($D_{50} 163.5 \pm 8.3 \mu\text{m}$) sediments (Table 1). Owing to its greater freshwater inputs, the Western Scheldt estuary generally has higher total dissolved inorganic nitrogen, phosphate and dissolved silica concentrations, though lower ammonium concentrations, than the Eastern Scheldt (Table 1).

2.3 Incubations and porewater extraction

Each station was visited once during low tide between August–October 2020. Sediment core samples were taken in triplicate for undisturbed nutrient exchange incubations (30 cm long cores, 15 cm inner diameter (\varnothing) filled with sediment to 50% of the core), and for pore water extraction (30 cm long cores, 10 cm \varnothing). Water (10 L) was collected from nearby the site. All cores were immediately transported to the Royal Netherlands Institute for Sea Research (NIOZ) after collection. Undisturbed incubation cores were filled with the unfiltered ambient water, aerated, and kept in a thermostatic bath at ambient water temperature in a dark controlled-climate room until the next day to acclimatize. The next day, the overlying water was renewed by carefully adding it to each sediment core preventing resuspension, the aeration was stopped, and the cores were closed with a hermetic lid with a central stirring mechanism that ensured the water was continuously homogenized. After closing the cores, the oxygen (O_2) concentration in the overlying water was continuously measured with an oxygen optode (Firesting, Pyrosience). The O_2 measurements were stopped when the concentration reached 70% saturation ($\sim 6 - 7$ h), after which lids were opened, and the overlying water was aerated to continue the incubation. Water samples (5-mL each) were filtered (Chromdis CA $0.45 \mu\text{m}$, 25 mm, No. 250425) for analysis of dissolved inorganic nitrogen (NH_4^+ , NO_2^- , NO_3^-), dissolved silicate (DSi) and PO_4^{3-} and were taken at the start of the incubation, at the end of the respiration measurement (6–7 h), and after 23, 31 and 48 hours.

The pore water cores were processed immediately after arrival to the NIOZ. The cores were sliced every 0.5 cm from 0 to 3 cm and

TABLE 1 Abiotic characteristics of the sediment (top 5 cm) and water column at the different sites of the Eastern Scheldt and Western Scheldt.

Site	S	High tidal zone		Low tidal zone		NH ₄ ⁺	NO ₂ ⁻	NO ₃ ⁻	DSi	PO ₄ ³⁻
		D50 μm	Por	D50 μm	Por					
Western Scheldt estuary										
AP ⁺	1	24.9 ± 2.8	0.8 ± 0*	–	–	47.5 ± 1.5	12.2 ± 0.2	291.2 ± 1.3	144.7 ± 4.6	8.1 ± 0.4
GBS	9	48.1 ± 9.6	0.8 ± 0.2	48.9 ± 3.4	0.7 ± 0.1	0.9 ± 0.9	0.3 ± 0	107.2 ± 11.6	44.7 ± 4.7	5.1 ± 0.5
RL	13	133.1 ± 7.8	0.5 ± 0.1	163.5 ± 8.3	0.4 ± 0.1	1.3 ± 0.6	1.5 ± 0	93.9 ± 0.8	46.2 ± 0.6	5.2 ± 0.1
ZG	30	62.2 ± 8.2	0.7 ± 0.1	51.7 ± 6.8	0.7 ± 0.1	9.6 ± 1.8	1.9 ± 0.1	28.1 ± 2.5	29.9 ± 14.4	2.6 ± 0.5
PP	30	53.9 ± 3	0.8 ± 0.2	72.3 ± 6.2	0.6 ± 0.1	15.8 ± 1.2	1.9 ± 0.1	21 ± 0.5	25.2 ± 2.3	2.3 ± 0.1
Mean						11.4 ± 14.3	2.6 ± 3.5'	87.9 ± 82.2'	48.5 ± 36.4'	4.3 ± 1.9'
Eastern Scheldt tidal bay										
DT	30	122.7 ± 18.3	0.5 ± 0.1	116.8 ± 1.5	0.5 ± 0.1	1.9 ± 1	0.2 ± 0.1	28.3 ± 1.9	18.4 ± 1	2 ± 0.1
RK	30	105 ± 4.3	0.5 ± 0.1	124.4 ± 4.6	0.5 ± 0.1	9.4 ± 0.8	0.4 ± 0	21.8 ± 0.8	15.6 ± 0.2	1.7 ± 0.3
ZK ⁺	30	83 ± 5.2	0.7 ± 0.1	–	–	0.5 ± 0.3	0.5 ± 0.5	30 ± 7.2	25.7 ± 0.3	1.8 ± 0.6
Mean						4.3 ± 4.1	0.3 ± 0.3	26.3 ± 4.7	19 ± 3.9	1.9 ± 0.3

* Porosity in Appels was >1 possibly caused by a sample manipulation error therefore porosity values from Rios-Yunes et al. (2023a) will be used instead.

+ Sites AP and ZK were only sampled in the high tidal zone.

Mean ± standard deviation of median sediment grain size (D50, μm), volumetric porosity (Por), and water-column salinity (S) and concentration of ammonium (NH₄⁺), nitrite (NO₂⁻), nitrate (NO₃⁻), dissolved silicate (DSi) and phosphate (PO₄³⁻) in mmol m⁻³. Sites in the Western Scheldt are ordered from upstream to downstream. Numbers marked with a (') represent a significant difference (t-test, p<0.05) between mean values in the WS and ES.

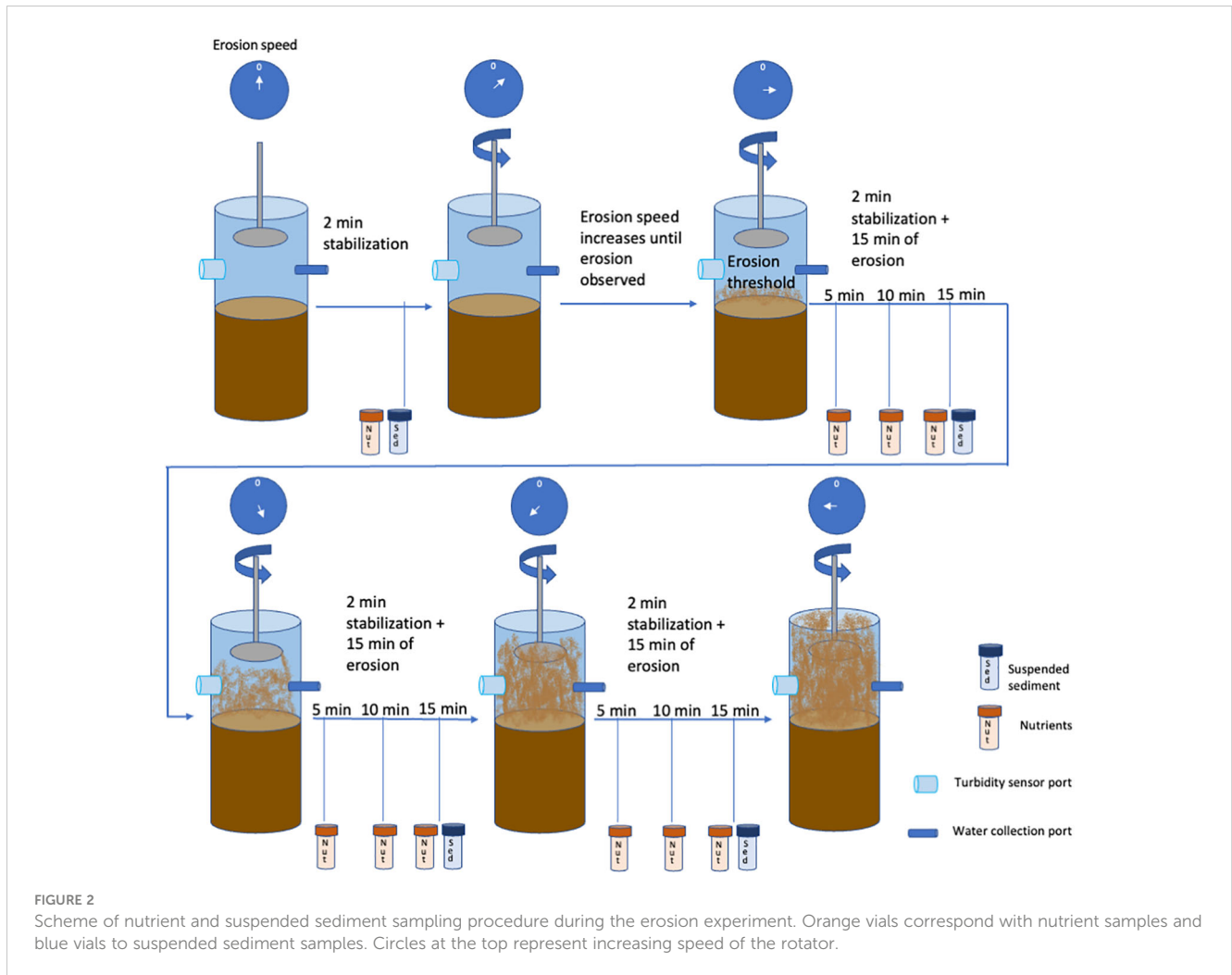
every 1 cm from 3 to 10 cm inside an anoxic glove bag. Half of each slice was transferred to a centrifuge filter tube with a basket (Chrom Tech, CTF-NY045-03) fitted with a glass fibre filter (Whatman GF/F, 0.7μm, 21 mm, WHA1825021). Pore water was extracted by centrifugation (10 min, 5000 rpm). Thereafter the samples were taken to an anoxic glove bag and an aliquot of 500 μL was obtained for NH₄⁺, NO₂⁻, NO₃⁻, and DSi; and one of 100 μL acidified with 10 μL of 1 M sulfuric acid (Merck, No. 100731) was used for PO₄³⁻ analysis.

2.4 Erosion experiment

Erosion experiments were conducted *in-situ* in triplicate at each location (high and low tidal zone) per site. A modified EROMES erosion chamber (37 cm long, 25 cm Ø, Appendix 2) with an open top and a rotating disc (Kalnejais et al., 2010) was placed on the sediment and inserted down to 15 cm in AP, and down to 10 cm in the other sites. Thereafter, water from the site was carefully added to avoid sediment resuspension. The chamber had a port for water sampling and another for a turbidity sensor which logged NTU values every 10 s (Turner Designs Cyclops 7F submersible sensor interfaced with a Turner Designs DataBank Handheld Datalogger) (Figure 2, Appendix 2). The turbidity sensor was calibrated prior to the sampling with 3 calibration standards of 10, 100 and 1000 NTU and one blank following the manufacturer protocols (Turner Designs, n.d). The

rotating disc was calibrated in the laboratory with an Acoustic Doppler Velocimeter (ADV, Nortek Vectrino Profiler) to obtain near-bed flow velocity and shear stress as a function of rotation speed.

The experimental set-up for the erosion experiment and sample collection procedure for nutrients (NH₄⁺, NO₂⁻, NO₃⁻, DSi and PO₄³⁻) and suspended sediments is shown in Figure 2. Initial water samples (nutrients and suspended sediments) were taken 2 min after the addition of water to account for any instantaneous release of nutrients that may have occurred upon the water addition. Then, the disc rotation was slowly increased until resuspension was detected with the turbidity sensor and erosion could be seen to occur across the entire surface of the core, i.e. the erosion threshold. From this point onwards, the rotation speed was incrementally increased until it was no longer possible to measure turbidity changes with the turbidity sensor, which typically happened at a maximum flow velocity between 0.175 m s⁻¹ and 0.203 m s⁻¹. Each rotation speed was held for 17 min allowing for 2 min of stabilization after which three water nutrient samples (5 mL filtered with Chromdis CA filter 0.45 μm, 25 mm, No. 250425; orange vials in Figure 2) were taken with a 5 min interval between them. The suspended sediments were sampled (40 mL) in the last interval (Figure 2, blue vial). Maximum erosion was determined when the SS concentration stabilized. Between three to five speed increments were imposed for each replicate. The range of imposed flow velocities was 0 m s⁻¹, 0.067 m s⁻¹, 0.106 m s⁻¹, 0.149 m s⁻¹, 0.175 m s⁻¹, and 0.203 m s⁻¹.



2.5 Sample analysis

Nutrient samples from the incubations, pore water and erosion experiment were collected in 6 ml plastic vials and stored at -20°C until analysis with a Segmented Flow Analyzer (QuAatro39 AutoAnalyzer with XY-2 Sampler Autosampler, SEAL Analytical) (Jodo et al., 1992). Detection limits were: 0.05 mmol m^{-3} for NH_4^+ and DSi, 0.03 mmol m^{-3} for NO_3^- and PO_4^{3-} and 0.01 mmol m^{-3} for NO_2^- . Sediment-water exchange fluxes of O_2 and inorganic nutrients (NH_4^+ , NO_2^- , NO_3^- , DSi and PO_4^{3-}) were estimated by linear regression of the concentration (mmol m^{-3}) versus time (d). The slope of the regression was multiplied by the height of the overlying water column (m) to obtain the flux in $\text{mmol m}^{-2} \text{ d}^{-1}$. The concentration of suspended sediment was calculated by resuspending the suspended sediment samples and filtering 10 ml of the sample with a pre-weighed GF/F filter (Whatman). Thereafter, the filters were dried for 48 h at 60°C and weighed. The weight difference was recorded as the suspended sediment weight. A regression between the discrete suspended sediment weight values and the NTU values from the turbidity sensor was made to calculate the suspended sediments concentration (SSC) during the experiment.

2.6 Statistical methods and data analysis

Linear models were used to test if sediment grain size or pore water nutrient concentrations could explain nutrient release by erosion. Statistical differences were detected with a t-test when the data distribution was normal, otherwise a Kruskal-Wallis test was used. Nutrient fluxes for each erosion speed were estimated by fitting a linear regression over the concentration versus time (5, 10, 15 minutes), and multiplying the slope of the regression by the height of the overlying water column. The thickness of eroded sediment (m) was calculated from the SSC as:

$$\text{Erosion depth} = \frac{sp * h}{\rho * (1 - \varphi)}$$

Where sp is the concentration of suspended particles (Kg m^{-3}), h is the height of the water column (m) inside the erosion chamber, ρ is the bulk density of the sediment defined as 2600 kg m^{-3} (Haan et al., 1994) and φ is the sediment porosity of the top 1 cm. From the eroded sediment depth, the total amount of pore water nutrients released into the water (C_{erosion} , mmol m^{-2}) was calculated as:

$$C_{\text{erosion}} = \text{Concentration}_{pw} * \text{Erosion depth} * \varphi \quad \text{Eq. 1}$$

Where $Concentration_{pw}$ is the concentration of pore water nutrients ($mmol\ m^{-3}$) in the top 1 cm of the sediment. The expected water column nutrient concentration (Nut_{exp} , $mmol\ m^{-3}$) due to nutrient release from sediment erosion (Eq. 1) and the undisturbed ambient nutrient flux at time t was calculated as:

$$Nut_{exp}(t) = Nut_{bw} + \frac{\int_0^t F_{release} dt + C_{erosion}(t)}{h + Erosion\ depth}$$

Where Nut_{bw} is the nutrient concentration in the water column at the start of the experiment ($mmol\ m^{-3}$), and the integral involving $F_{release}$ is the undisturbed nutrient flux ($mmol\ m^{-2}$) calculated from the sediment incubation over the duration (d) of the experiment.

Data analysis, visualization and statistical tests were done using R (R Core Team, 2020). Geospatial analysis was conducted with the program QGIS (QGIS Development Team, 2021).

3 Results

3.1 Oxygen and nutrient fluxes from undisturbed sediments

In general, all fluxes (O_2 , NH_4^+ , NO_2^- , NO_3^- , DSi and PO_4^{3-}) showed significant differences between high ($_{high}$) and low ($_{low}$) tidal

zones (Appendix 3) except for RK in the Eastern Scheldt. The O_2 consumption rate in stations in the high tidal zone of the Western Scheldt increased from the freshwater site (AP) ($-42 \pm 5.1\ mmol\ m^{-2}\ d^{-1}$) to the sandy brackish station (RL_{high}) ($-73.4 \pm 7.7\ mmol\ m^{-2}\ d^{-1}$) and then decreased seawards (PP_{high}) ($-60.2 \pm 6.4\ mmol\ m^{-2}\ d^{-1}$, Table 2). All stations except ZG_{high} showed an efflux (directed out of the sediment) of NH_4^+ (0.8 ± 1.3 to $5.3 \pm 1\ mmol\ m^{-2}\ d^{-1}$) and an influx of NO_3^- (-1 ± 0.2 to $-4.6 \pm 0.2\ mmol\ m^{-2}\ d^{-1}$, Table 2). The freshwater site exhibited an influx of PO_4^{3-} ($-0.2 \pm 0.1\ mmol\ m^{-2}\ d^{-1}$) and DSi ($-0.2 \pm 0.2\ mmol\ m^{-2}\ d^{-1}$) that became an efflux in the brackish and marine parts of the Western Scheldt. In the low tidal zone O_2 consumption was higher in marine ($> -61.4 \pm 7.5\ mmol\ m^{-2}\ d^{-1}$, PP_{low}) than in brackish stations (GBS_{low} and RL_{low}). All stations in the low tidal zone, apart from ZG_{low} , exhibited an influx of NO_3^- that ranged between -0.9 ± 0.1 and $-3.4 \pm 0.3\ mmol\ m^{-2}\ d^{-1}$ (Table 2). Similarly, an efflux of DSi was observed in all stations (max. $6.5 \pm 0.8\ mmol\ m^{-2}\ d^{-1}$, ZG_{low}) except for RL_{low} .

Overall, the flux of PO_4^{3-} in the freshwater site was significantly different from the other sites; and it was the only significantly different flux between the fresh and brackish sites (Appendix 4). Fluxes at the brackish sites, GBS and RL, did not differ significantly. However, the flux of NO_3^- and DSi was significantly different between fresh and brackish sites and the marine sites (Appendix 4).

In the Eastern Scheldt, the muddy station ZK_{high} had the highest O_2 consumption ($-55.6 \pm 3.45\ mmol\ m^{-2}\ d^{-1}$), and the sandy DT_{low} the lowest ($-23.2 \pm 2.8\ mmol\ m^{-2}\ d^{-1}$) (Table 2). All stations in the

TABLE 2 Mean \pm standard deviation of oxygen and nutrient fluxes ($mmol\ m^{-2}\ d^{-1}$) at the high and low tidal zone locations of the different sites in the Western and Eastern Scheldt.

Location	Site	O_2	NH_4^+	NO_2^-	NO_3^-	DSi	PO_4^{3-}
Western Scheldt estuary		mmol $m^{-2}\ d^{-1}$					
High tidal zone	AP	-42 ± 5.1	2.6 ± 0.2	0.1 ± 0	-4 ± 0.3	-0.2 ± 0.2	-0.2 ± 0.1
	GBS	-49.4 ± 7.1	0.8 ± 1.3	0 ± 0	-2.7 ± 0.9	2 ± 0.8	0.2 ± 0.1
	RL	-73.4 ± 7.7	3.8 ± 0.8	0.2 ± 0	-4.6 ± 0.2	4.2 ± 0.7	0.2 ± 0
	ZG	-68.4 ± 5.4	-0.1 ± 0.2	-0.1 ± 0	0 ± 1.2	5.2 ± 0.2	0.1 ± 0.1
	PP	-60.2 ± 6.4	4 ± 0.3	0.2 ± 0.1	-1 ± 0.2	4.9 ± 0.3	0 ± 0
Low tidal zone	AP	–	–	–	–	–	–
	GBS	-35.8 ± 11.4	1.4 ± 0.4	0.1 ± 0.1	-3.4 ± 0.3	1.6 ± 0.7	0.1 ± 0
	RL	-33.7 ± 10.9	1.2 ± 0.7	0 ± 0	-3 ± 0.7	-0.7 ± 0.3	0 ± 0
	ZG	-83.3 ± 7.4	2.3 ± 0.5	0 ± 0	0.9 ± 0.6	6.5 ± 0.8	0.1 ± 0
	PP	-61.4 ± 7.5	5.3 ± 1	0.3 ± 0.1	-0.9 ± 0.1	4.2 ± 0.6	0 ± 0
Eastern Scheldt tidal bay							
High tidal zone	DT	-34 ± 8.4	2.6 ± 1	0.1 ± 0	-0.8 ± 0.4	-0.1 ± 0.1	-0.1 ± 0
	RK	-28.3 ± 0.7	3.7 ± 0.7	0 ± 0	-0.7 ± 0.1	-0.5 ± 0.1	0 ± 0
	ZK	-55.6 ± 3.5	2.4 ± 0.4	0 ± 0	-1.4 ± 0.4	2.5 ± 0.2	0 ± 0.1
Low tidal zone	DT	-23.2 ± 2.8	1.1 ± 0.8	0 ± 0	-0.5 ± 0.2	-0.2 ± 0.1	-0.1 ± 0
	RK	-35 ± 2.6	3.3 ± 0.3	0 ± 0	-1 ± 0.1	0.1 ± 0	0 ± 0
	ZK	–	–	–	–	–	–

Sites in the Western Scheldt are ordered from upstream to downstream. A negative sign (-) indicates an influx and a positive (+) sign an efflux from the sediment into the water column.

Eastern Scheldt tidal bay had an efflux of NH_4^+ which was highest in RK_{high} ($\text{max } 3.7 \pm 0.7 \text{ mmol m}^{-2} \text{ d}^{-1}$), and an influx of NO_3^- that was greatest in ZK ($-1.4 \pm 0.4 \text{ mmol m}^{-2} \text{ d}^{-1}$). Sandy sites (DT and RK_{high}) exhibited an influx of DSi, while muddy ZK an efflux ($2.5 \pm 0.2 \text{ mmol m}^{-2} \text{ d}^{-1}$). All stations except RK_{high} had an influx of PO_4^{3-} . The flux of NH_4^+ was significantly different between RK and DT (Appendix 4). The muddy site ZK exhibited significantly different fluxes of NO_3^- to DT, and DSi to DT and RK.

Between systems, oxygen consumption rates, the efflux of DSi, and the influx of NO_3^- were significantly higher (t-test, $p \leq 0.05$, Appendix 5) in the Western Scheldt (all sites) than in the Eastern Scheldt. Phosphate flux was significantly different (t-test, $p \leq 0.05$) in the Eastern Scheldt (net influx) and the WS (net efflux). In contrast, fluxes of NH_4^+ and NO_2^- were not significantly different between systems. Comparing only the marine Western Scheldt sites (ZG and PP) with the Eastern Scheldt, the significant differences in O_2 , NO_3^- , DSi and PO_4^{3-} fluxes were retained (t-test, $p \leq 0.05$, Appendix 6).

3.2 Pore water nutrients

In all pore water profiles, the concentration of NH_4^+ was lowest in the surface 0-1 cm and increased with sediment depth, while the concentration of NO_2^- and NO_3^- was high near the surface and decreased with depth (Figures 3A–C, F–H, K–M, P–R, U–W). Most sites of the Western Scheldt showed comparable concentrations of NH_4^+ and NO_2^- except for the freshwater site which had the highest concentration of NH_4^+ (up to 1000 mmol m^{-3}) and NO_2^- , and RL_{low} with the lowest concentration of NH_4^+ . The concentration of NO_3^- in the Western Scheldt sediments varied more between sites and locations, with the highest (ZG_{high}) and the lowest (ZG_{low}) concentrations occurring in the marine section. DSi increased with depth and was similar at all stations, except for RL_{high} which was significantly lower (Wilcoxon rank sum test, $p \leq 0.05$, Figures 3D, I, N, S, X). In the low tidal zone, the highest concentration of DSi was observed in ZG_{low} and GBS_{low} , and the lowest in RL_{low} . Phosphate concentrations did not exhibit a consistent trend with sediment depth, but the Western Scheldt locations of AP, GBS_{low} , ZG_{high} , and PP_{high} and low had subsurface peaks below 2 cm. Overall, the pore water concentration of NH_4^+ and PO_4^{3-} decreased from the fresh to the brackish and the marine parts of the estuary while the concentration of NO_3^- increased.

In the Eastern Scheldt, ammonium also increased with sediment depth with the highest concentration observed in the sandy site RK_{high} and the lowest at RK_{low} (Figure 3A, E). NO_3^- was highest in DT_{high} and lowest in RK_{low} (Figure 3AB, AG). The highest concentration of DSi and PO_4^{3-} was observed in RK_{high} reaching over 500 and 300 mmol m^{-3} , respectively. No correlation was found between pore water nutrient concentration and grain size except for DSi ($p \leq 0.05$, $R^2 = 0.87$) and PO_4^{3-} ($p \leq 0.05$, $R^2 = 0.67$) in the low tidal zone.

3.3 Sediment resuspension and solute release

A small amount of sediment particles in suspension was visually observed at the beginning of the erosion experiment at

all sites, however, this minor resuspension was too low to influence the critical erosion threshold (Appendix 7). The freshwater site exhibited the lowest erosion threshold speed ($\leq 0.067 \text{ m s}^{-1}$), while for all other sites the threshold speed fluctuated between 0.106 and 0.149 m s^{-1} . Once the erosion threshold was exceeded, the concentration of suspended particles increased with increasing velocity until the SSC stabilized (Figure 4A). However, in the freshwater site the SSC seemed to plateau faster than in other stations like RL and DT where the concentration stabilized towards the end of the experiment (Figures 4C, G). In all other stations the SSC increased steadily during the erosion experiment. The SSC and erosion depth observed at the highest erosion speed differed between sites and went from as little as 0.62 Kg m^{-3} , corresponding to 0.25 mm erosion in GBS_{200} (0.203 m s^{-1}) to as much as 33.85 Kg m^{-3} with an erosion depth of 6.1 mm in RL_{high} (0.175 m s^{-1}) (Appendix 7).

The erosion of sediments induced nutrient release in most sites, except for PO_4^{3-} in the Eastern Scheldt. In the WS, the freshwater site AP, showed an increase in concentration (blue dots in Figures 4I, Q) of NH_4^+ , NO_2^- that was twice as high as the estimated increase due to release of pore water caused by erosion (grey columns), but for PO_4^{3-} the expected concentration was closer to the observed increase (Figure 4Y). In other WS sites (ZG_{high} , and PP_{low}), the observed concentration of NH_4^+ and that of PO_4^{3-} for GBS_{high} and low , RL_{high} and PP_{high} and low was higher than expected from pore water release, while the concentration of NH_4^+ in RL_{high} , ZG_{low} and PP_{high} and PO_4^{3-} in ZG_{low} matched the predicted release from pore water dilution (Figure 4).

In the Eastern Scheldt, the observed increase in concentration of NH_4^+ and NO_2^-) closely matched the predicted concentrations due to release from pore water nutrients in DT_{high} (grey bars in Figure 4N, V). In contrast, the release of NH_4^+ in DT_{low} and ZK_{high} was lower than predicted by pore water dilution (grey bars in Figures 2AD, O). The locations RK_{high} and low exhibited a sharp increase in the concentration of NH_4^+ and NO_2^- during erosion which was several times higher than expected by pore water release only. Changes in the water column concentration of PO_4^{3-} in the Eastern Scheldt showed an interesting pattern with the concentration sharply decreasing with erosion at all sites and following the opposite direction of the release expected from pore water dilution (Figures 4AD, AE, AF, BC, BD). No correlation was found between nutrient release and grain size.

A comparison was made between the undisturbed and the erosion fluxes of NH_4^+ , NO_2^- and PO_4^{3-} to determine the contribution of sediment erosion to the overall nutrient fluxes (Figure 5). Sediment erosion had an additive effect on the undisturbed flux when both the undisturbed and the erosion fluxes were an efflux or an influx. In those instances, an hour of erosion fluxes was equivalent to several days of undisturbed PO_4^{3-} , NO_2^- and NH_4^+ fluxes in 93%, 69% and 19% of cases, respectively (Appendix 8). Other cases showed an inversion in the direction of the erosion fluxes compared to the undisturbed fluxes. In those instances, an hour of sediment resuspension counterbalanced at least a day of undisturbed fluxes in 95%, 55% and 20% of cases for PO_4^{3-} , NO_2^- and NH_4^+ , respectively (Appendix 8).

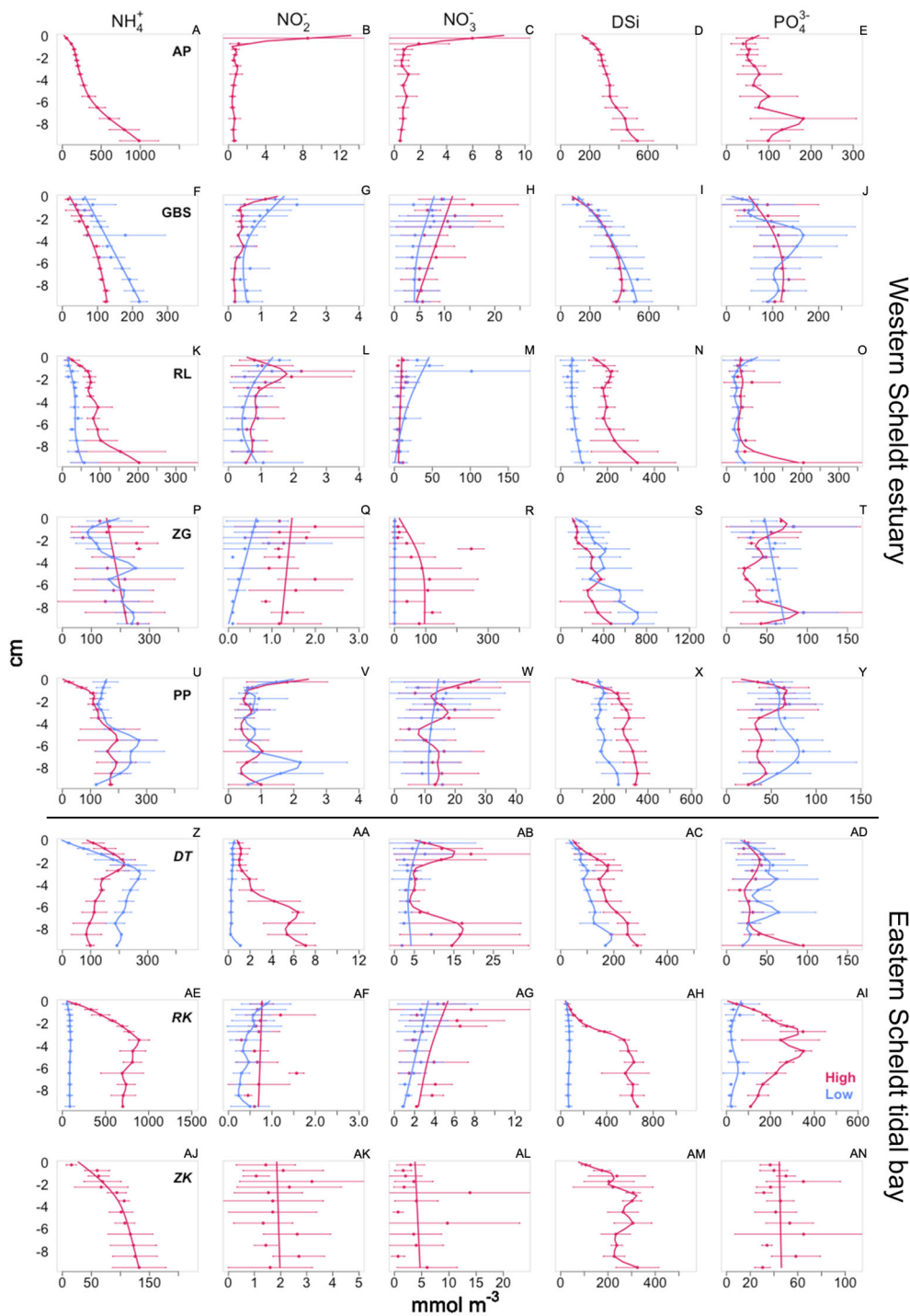


FIGURE 3
 Pore water profiles from the high (red) and low (blue) tidal zone from the Western (A–Y) and Eastern Scheldt (W–AN) sites. Dots and horizontal lines represent mean ± standard deviation of pore water concentration. Vertical line is a smoothed spline. Western Scheldt site are ordered from upstream to downstream. Notice differences in x axis scales.

4 Discussion

Our results show a differential response to sediment resuspension and nutrient release of adjacent coastal systems. The nutrients ammonium and nitrite responded predictably to sediment

erosion by increasing their concentration in both systems. In contrast, the concentration of phosphate increased with nutrient erosion in the estuarine system, but not in the tidal bay where it decreased. The concentration of nitrate appeared to be unaltered by sediment erosion.

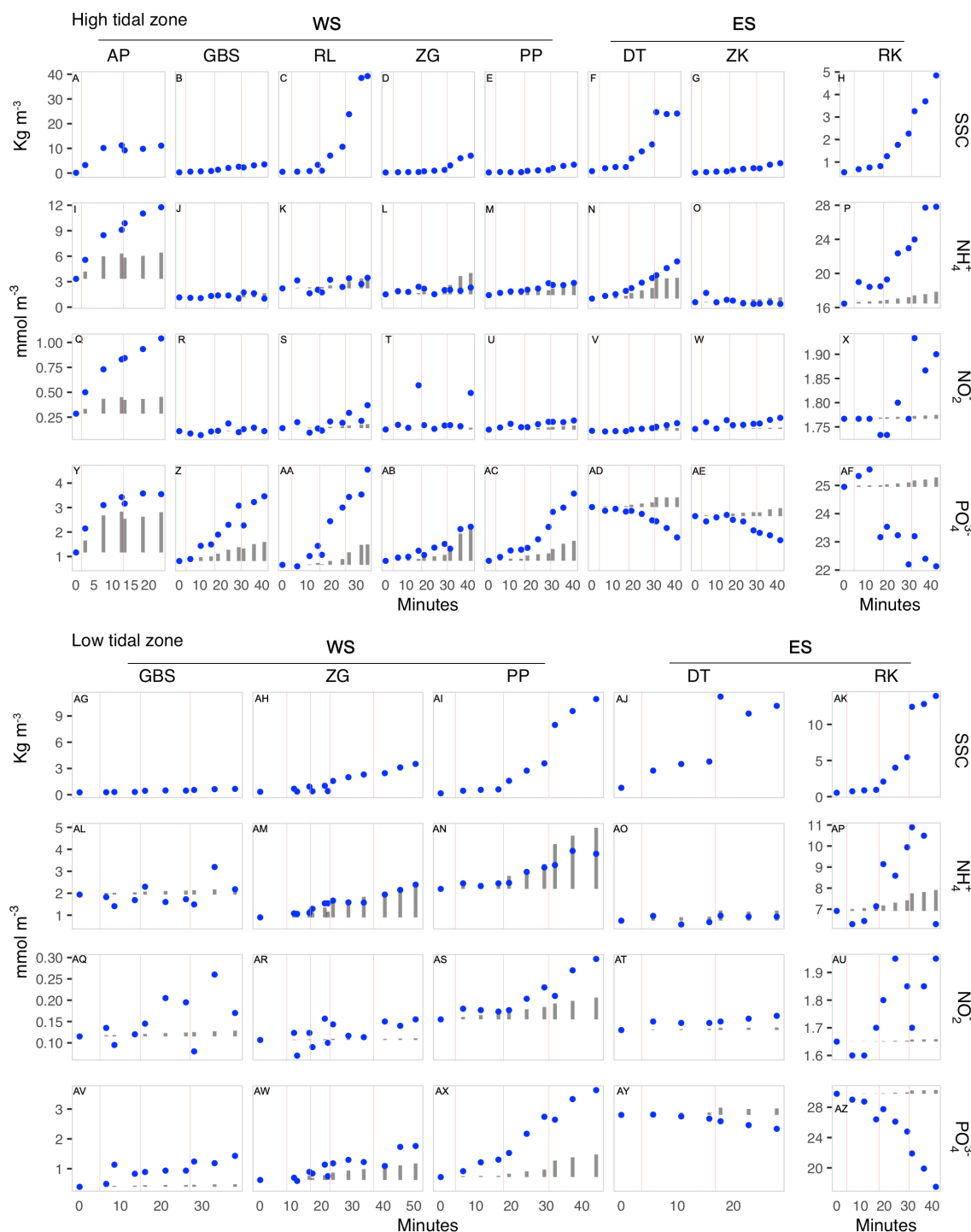


FIGURE 4
 Nutrient release and suspended sediment concentration (SSC) changes due to sediment erosion over time in the high (A–AF) and low (AG–AZ) tidal zone locations of the Eastern (ES) and Western Scheldt (WS). All nutrient concentrations expressed in mmol m⁻³. Suspended sediments concentration in Kg m⁻³. Blue dots denote measured nutrient concentrations during the erosion experiment. Grey bars indicate the bottom water concentration at the beginning of the experiment (t₀) plus the predicted increase in concentration solely from dilution of pore water nutrients from the eroded layer of top sediments, as calculated from the suspended particles concentration. Red lines indicate the moments at which the speed was increased during the experiment. Western Scheldt sites AP, GBS, RL, ZG, and PP are ordered from upstream to downstream sites.

4.1 Physicochemical characteristics

The WS exhibits the typical characteristics of an “estuarine filter” with a decrease in the concentration of nutrients in the water

column from the freshwater area to the mouth (Table 1). This gradient has been well documented (Middelburg and Nieuwenhuize, 2000; Soetaert et al., 2006; Rios-Yunes et al., 2023a) and results from the dilution of land runoff in riverine

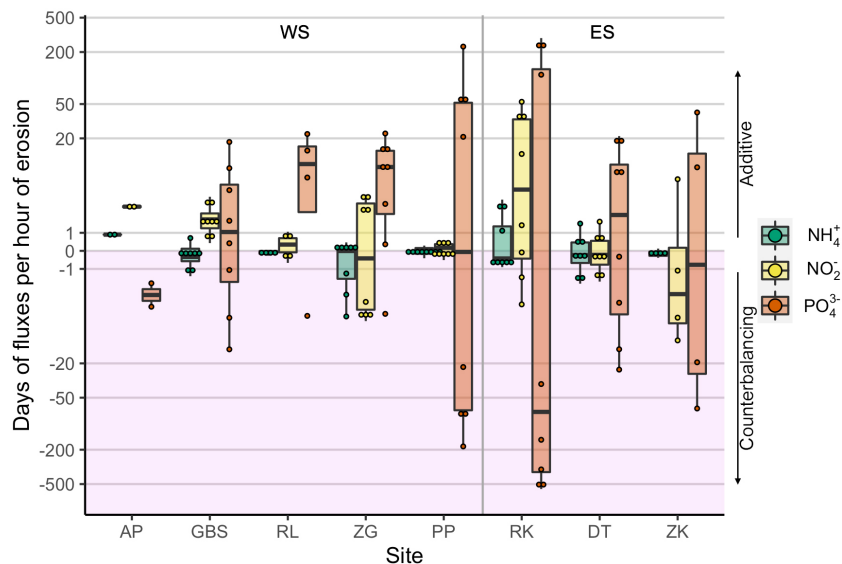


FIGURE 5

Equivalence of one hour of erosion to days of undisturbed fluxes. All replicates of both the high and the low water line locations are pooled together by nutrient per site. The additive effect of erosion on the undisturbed fluxes is shown in the white area with positive values, while the cases with a counterbalancing effect are depicted in the shaded area with negative values. Vertical line separates between WS sites arranged from fresh to marine salinities and sites in the ES. Notice the logarithmic scale in the y axis.

water with seawater (Gilbert et al., 2007), biogeochemical transformations along the estuary (e.g. sorption, denitrification, etc.) (Soetaert et al., 2006; Rios-Yunes et al., 2023a) and uptake by both marine and terrestrial (e.g. adjacent reed marshes) primary producers (Struyf et al., 2005; Arndt et al., 2009). The Eastern Scheldt is, in contrast, a tidal bay with a single connection with the North Sea *via* the storm surge barrier. This unilateral tidal exchange though this inlet is reported to cause decreasing concentrations of nutrients and increased water retention towards the eastern section (Jiang et al., 2019). However, we were not able to detect this gradient based on our results.

4.2 Sediment oxygen consumption and undisturbed nutrient fluxes

Sediment oxygen consumption and nutrient fluxes are indicative of the activity and nature of the biogeochemical processes occurring within the sediment such as OM mineralization, respiration, and primary production. The 'undisturbed' fluxes were measured to determine the activity of the sediment and to compare them with the nutrient fluxes observed during the erosion experiment. Fluxes can be detected as an influx when processes (or organisms) within the sediments consume substances from the water column that are not produced in the sediment, such as oxygen, or when organisms utilize the totality of nutrients released during mineralization plus some nutrients from the water column. Alternatively, an efflux is observed when nutrients released from sedimentary OM mineralization are not entirely consumed by benthic processes but rather escape to the water column *via* diffusion, bioturbation, and bio-irrigation.

The increase in O_2 consumption along the salinity gradient of the Western Scheldt (Table 2) may result from increasing rates of oxygen consuming processes like aerobic respiration and nitrification from fresh to marine areas, as well as changes in the macrofaunal community (Ysebaert et al., 1993; Mestdagh et al., 2020). Nutrient retention also changes through the estuary with freshwater sediments acting as a sink of PO_4^{3-} , which is significantly different to all other sites (Appendix 4). Similarly, brackish sediments, and to a lesser extent freshwater sediments, exhibit an important influx of NO_3^- implying high rates of denitrification (Table 2). Nitrogen dynamics in the fresh and brackish areas are different to marine sites (Appendix 4). These results are consistent with a recent analysis of Western Scheldt sediments by Rios-Yunes et al. (2023a), where freshwater sediments were recognized as a sink of phosphate facilitated by sorption to sediments; and brackish sediments were a sink of nitrogen due to enhanced denitrification.

In the Eastern Scheldt, the muddy site of ZK showed the highest oxygen consumption rates, and likely also had higher denitrification rates compared to the other ES sites, as evidenced by the prevalent influx of NO_3^- (Table 2). The lower O_2 consumption and smaller fluxes of NO_3^- observed in DT and RK (Table 2) may have resulted from their coarser grain sizes that facilitated tidal flushing of OM, limiting mineralization and nitrification (Precht et al., 2004). The influx of NO_3^- in DT was significantly lower than in ZK (Appendix 4) suggesting that nitrification may have been lowest in this site.

A comparison of Eastern Scheldt (all sites) and WS (ZG and PP) sites evidenced significantly higher O_2 consumption in the Western Scheldt (Appendix 6, t-test, $p \leq 0.05$). Both systems receive autochthonous input from phytoplankton and, from the more dominant, microphytobenthos production, but the Western Scheldt also has a permanent influx of allochthonous OM from

rivers and the North Sea which contributes to the supply of OM thereby fueling higher mineralization rates (mean $68.3 \text{ mmol m}^{-2} \text{ d}^{-1}$). In contrast, the Eastern Scheldt has a small net input of OM from the North Sea, longer residence times, and intense OM grazing in areas with a high biomass of filter-feeders (Jiang et al., 2020), which results in lower benthic O_2 consumption in the intertidal sites (mean $35.2 \text{ mmol m}^{-2} \text{ d}^{-1}$, Appendix 6).

In estuaries, phosphate sorption decreases with increasing salinity and generally, an efflux of phosphate from the sediment is observed in brackish and marine areas (Table 2) (Jordan et al., 2008; Rios-Yunes et al., 2023a). The flux of PO_4^{3-} is also influenced by the concentration of phosphate in the water column; the pore water concentration of N, DSi, and sulphur as well as by an interplay between rates of sulfate reduction and concentration, or turnover, of iron oxides (FeOOH) (Caraco et al., 1990; Slomp et al., 1996; Jordan et al., 2008). The significantly different (t-test, $p \leq 0.05$) PO_4^{3-} fluxes between the marine Eastern Scheldt ($-0.04 \text{ mmol m}^{-2} \text{ d}^{-1}$) and marine sites (PP and ZG) in the Western Scheldt ($0.05 \text{ mmol m}^{-2} \text{ d}^{-1}$, Appendix 5) could not have been attributed to the effect of salinity. It was similarly unlikely that the disparities in fluxes were related to differences in concentration of PO_4^{3-} in the water column (Western Scheldt 2.4 mmol m^{-3} and Eastern Scheldt 1.9 mmol m^{-3} , $p \leq 0.05$; Appendix 6), or in the pore water of the upper cm of the sediment (58.8 mmol m^{-3} in the Western Scheldt and 56.0 mmol m^{-3} in the Eastern Scheldt, $p = 0.2$, Appendix 5), given the small differences. It is, however, possible that the observed differences are associated with physicochemical processes in the sediment such as sorption-desorption (Jordan et al., 2008), but we are unable to provide a conclusion based on the available data. It is noteworthy that these observations were obtained in the summer-autumn, so it is possible that the dynamics would be different in other seasons.

4.3 Pore water nutrients

The remineralization of OM releases nutrients (e.g. NH_4^+ , DSi, and PO_4^{3-}) that can be transformed and stored within the sediment or released into the water column (Slomp et al., 1996; Herbert, 1999; Struyf et al., 2005; Jordan et al., 2008). In the Western Scheldt, the fresh water (AP) and brackish (GBS) sites are within the vicinity of *Phragmites australis* reed marshes which are known to store biogenic silicate (BSi) in the form of phytoliths (Struyf et al., 2005). The observed accumulation of DSi at depth (Figure 3) could be associated with the transfer and burial of reed OM from the marsh to the mudflat and subsequent dissolution of BSi (Struyf et al., 2005). The decrease in pore water concentration of NH_4^+ and the increase of NO_3^- from the fresh to the brackish and the marine parts of the Western Scheldt estuary (Figure 3) may be related to the deeper penetration of oxygen in coarser sediments that promotes nitrification.

In contrast, the decreasing pore water concentration of PO_4^{3-} with increasing salinity is most likely associated with the differential sorption of phosphate to oxidized iron and sediment particles along salinity gradients (Jordan et al., 2008), but it could also be influenced by the presence of silicates, ammonium, iron, and oxygen (Caraco et al., 1990; Tengberg et al., 2003; Morgan et al.,

2012), as well as the composition of the sediment particles (Borggaard, 1983). Similar observations on the concentration of pore water nutrients the Western Scheldt have been reported by Rios-Yunes et al. (2023a). It is noteworthy that the WS receives runoff from heavily farmed areas (Gilbert et al., 2007), so it is possible that the high porewater nutrient concentration in upstream sediments could also be associated with the historical accumulation of nutrients from land runoff (Shaughnessy et al., 2019). We are unaware of any existing data reporting on this.

In the Eastern Scheldt, the concentration of NH_4^+ and PO_4^{3-} increases steadily up to $\sim 3 \text{ cm}$ depth. This may be related to a deeper oxygen penetration depth that promotes OM mineralization within the top 3 cm, possibly facilitated by tidal flushing (Precht et al., 2004) or by bioturbation and bioirrigation (De Borger et al., 2020) in these sites. The low pore water nutrient concentrations observed in RL_{low} (Western Scheldt) and RK_{low} (Eastern Scheldt) may be associated with their coarse sediment grain size as this would allow tidal flushing of solutes (Precht et al., 2004).

4.4 Nutrient release by erosion

The differences in critical erosion threshold between sites are mostly associated with the intrinsic characteristics of the sediment (e.g. density, grain size, clay and organic matter content etc.) (Shrestha et al., 2001; Tang et al., 2020), but also with the presence of microphytobenthos that can stabilize surface sediment particles by excreting exopolymeric substances (Paterson et al., 2018), and with bioturbation which can destabilize the sediment matrix (Widdows et al., 2000a; Widdows et al., 2000b; Li et al., 2017). Nevertheless, the values obtained in our study were within values observed in other macrotidal systems like the Ems-Dollard, NL (between 0.1 and 0.6 N m^{-2}) (Kornman and Deckere, 1998; Dyer et al., 2000), but lower than those of, for example, the Humber estuary, UK ($\sim 0.4 \text{ N m}^{-2}$) (Amos et al., 1998).

Our field observations revealed that sediment resuspension in muddy sediments happened quickly when the upper unconsolidated layer was eroded. However, the resuspension plateaued with an increasing shear stress speed that failed to erode the consolidated sediment layer at greater depth. The freshwater site of AP in the Western Scheldt is characterized by an unconsolidated sediment layer on the sediment surface. This layer was easily eroded as evidenced by the low critical erosion speed needed to initiate erosion (0.067 m s^{-1}) and the rapid stabilization of the SSC (Figure 4). Different to muddier sediments, sites with coarser grain sizes, e.g. RL and DT, produced the highest concentration of suspended sediments (Appendix 7). In such sites, sediment resuspension continued until plateauing at higher erosion speeds (Figure 4). This stabilization likely occurred because the maximum concentration of particles in suspension was reached, and particle sedimentation was in balance with sediment erosion.

As sediments erode, dissolved solutes in pore water and sediment particles mix into the overlying water changing the concentration of dissolved nutrients NH_4^+ , NO_2^- and PO_4^{3-} (Figure 4). An increase in nutrient concentrations in the water

column may not only indicate a release of pore water nutrients, but also desorption of nutrients. A decrease in concentration is likely associated with the uptake of water column nutrients by sorption to suspended sediment particles or to other nutrients (Kalnejais et al., 2010; Morgan et al., 2012). It could also be caused by biological uptake, but this is unlikely to have occurred in our experiment since its duration was about 1 hour and thus changes caused by biological uptake would have been negligible.

Changes in the concentration of nutrients began slowly but increased with the speed of erosion and the duration of resuspension treatments. This was expected since pore water nutrients were being released, but also because the added particles in the water column had sufficient time to desorb nutrients, similar to findings from Niemistö and Lund-Hansen (2019). Moreover, changes in nutrient concentrations continued despite the apparent stabilization of the SSC (AP, DT, RL in Figure 4) further supporting the suggestion that suspension time is a more important factor for nutrient desorption than the number of particles.

In most sites, the nutrient concentration measured in the water column was greater than the expected pore water release from erosion (Figure 4). The difference between measured and expected concentration of the different nutrients is likely caused by reactions with the solid phase (i.e. desorption) (Falcão and Vale, 1995; Cabrita et al., 1999; Morin and Morse, 1999; Kalnejais et al., 2010; Morgan et al., 2012; Chen et al., 2018). The mismatch between expected input from pore water nutrients release and changes in the overlying water concentration (Figure 4) could also be the result of pore water entrainment from deeper layers of the sediment. Nevertheless, this seems implausible. First, because the sediments were rather muddy (except in sandy RL) with low permeability and porewater advection (Precht et al., 2004), and second, because previous reports have not found significant differences in pore water profiles before and after erosion events in fine-grained sediments (Kalnejais et al., 2010).

Changes in the overlying water concentration of ammonium and nitrate have been associated with ammonium oxidation (Niemistö et al., 2018). However, this process was observed after several hours of resuspension and caused the simultaneous increase of nitrates and decrease of NH_4^+ (Niemistö et al., 2018). In our case, it is unlikely that significant ammonium oxidation occurred in the erosion experiment because the duration of each erosion run was shorter than needed for the oxidation reaction to strongly affect ammonium or nitrate concentrations. Nevertheless, if there had been oxidation of NH_4^+ to NO_3^- it is possible we may not have detected it due to the high concentration of NO_3^- in the water column (Table 1) compared to pore waters in the surface (Figure 3). Other processes that gain relevance over longer periods of sediment resuspension and contribute to nitrogen transformation include ion-exchange reactions, and slow desorption processes (Kalnejais et al., 2010; Niemistö and Lund-Hansen, 2019) as well as biological uptake.

A surprising observation was the differential behavior of PO_4^{3-} between the Western Scheldt and Eastern Scheldt during the erosion experiment (Figure 4). In the Western Scheldt, phosphate was released with increasing erosion speed, at all stations, likely due to pore water addition to the water column combined with

desorption. Similar increases in PO_4^{3-} concentration attributed to desorption have been observed in North Sea subtidal sediments (Couceiro et al., 2013), the Boston Harbor, US (Kalnejais et al., 2010) and the Peel-Harvey Estuary, Aus. (Morgan et al., 2012). In contrast, sediment erosion decreased the concentration of phosphate in the water column of ES sites, therefore highlighting sediment resuspension as a possibly important process for PO_4^{3-} removal in this system. A decrease in phosphate with erosion has also been observed in North Sea sediments (Tiano et al., 2021), the Baltic Sea (Tengberg et al., 2003; Niemistö et al., 2018) and Great Bay estuary, US (Percuoco et al., 2015).

The differences in release or sorption of phosphate between the Western Scheldt and the Eastern Scheldt (Figure 4) are unlikely to be determined by the origin of their sediments since both systems have a similar geological history. Likewise, salinity can be ignored since the different phosphate dynamics were observed in sites with marine salinities. It is, however, possible that differences in, for example, iron oxide concentration may be the cause. Unfortunately, based on available data it is not possible to confidently determine the source of the different phosphate dynamics due to erosion.

The concentration of NO_3^- and DSI in the overlying water was one to two orders of magnitude higher than in pore waters in the top 1 cm of the sediment. Therefore, it is possible that the high concentrations in the water column masked the dilution of pore water nutrients appearing unaltered by increasing sediment erosion. Our results contrast with studies reporting an increase in overlying water concentrations of NO_3^- and DSI upon sediment resuspension in systems like the Boston Harbor, US (Kalnejais et al., 2010), the North Sea (Couceiro et al., 2013) and the Baltic Sea (Niemistö and Lund-Hansen, 2019), but also in the ES (Tiano et al., 2021). The disparity in DSI release between our study and that of Tiano et al. (2021) may result from their resuspension of 3 cm versus the 2 to 6 mm (Appendix 6) obtained in our erosion study.

No changes in DSI were detected by solely investigating fluctuations in the overlying water nutrient concentration. Nevertheless, it is possible that an erosion disturbance of > 2 cm depth like those previously reported in the Western Scheldt and Eastern Scheldt (de Vet et al., 2020) may cause DSI release as observed by Tiano et al. (2021) and possibly change the concentration of DSI in the overlying water.

4.5 Relevance of erosion mediated nutrient release

An erosion event can have an additive or counterbalancing effect on undisturbed nutrient fluxes as was evidenced by the comparison between undisturbed and erosion fluxes (Appendix 8). In both the additive and counterbalancing cases, however, the effects of resuspension obtained for PO_4^{3-} were one, and in for example PP and RK, up to three orders of magnitude higher than for NO_2^- and NH_4^+ (Figure 5). The larger effects on PO_4^{3-} release from resuspension were observed in PP and RK and are unlikely to be related to grain size characteristics as there was no correlation found between grain size and nutrient release. Instead, they are probably due to a lower exposure to wave action, as both sites are in

a sheltered position from the prevailing southwestern wind (de Vet et al., 2020), and/or to the high stability of these sediments as evidenced by their low long-term and daily fluctuations in bed level (Appendix 9). It is therefore plausible that the reduced frequency of resuspension events allows for the accumulation of pore water nutrients. These accumulated nutrients can subsequently be exchanged in case of a resuspension event; a similar observation has been reported by Abril et al. (1999). In this respect, it is likely that an erosion event would translate in greater nutrient exchange in sheltered sediments than in exposed areas where sediment resuspension and nutrient exchange are more regular. Moreover, the first erosion event is expected to cause a greater exchange than subsequent ones because each event would mobilize the nutrients stored since the last resuspension event.

The results obtained in the Eastern Scheldt sites DT and ZK can be compared with those of Tiano et al. (2021), who performed similar experiments at these sites. Our results coincide on the overall additive effect of erosion on undisturbed NH_4^+ fluxes in DT and ZK, however, they observed a greater effect of erosion on this flux, possibly due to a difference in methodology as they resuspended down to 3 cm depth. Regarding PO_4^{3-} , our observations also agree in that sediment resuspension had an additive effect on the influxes in DT and a counterbalancing one in ZK, however, these effects were higher in our experiment.

The relevance and magnitude of a storm event on intertidal areas erosion would depend on the wind direction and speed (de Vet et al., 2020) as they determine which areas are directly exposed to wave and wind action; the different hydrodynamic forces (Yang et al., 2003) together with duration and period of the tidal cycle (Green and Coco, 2014; de Vet et al., 2020) since they control the intensity of erosion and concentrate the effects of a storm in a certain area; and on the depth of the eroded layer. Other important aspects to be considered are seasonality (Bancón-Montigny et al., 2019) as well as precipitation and run off (Chen et al., 2018) because annual fluctuations may alter the effect of an erosion event; and land use of the surrounding area (Gilbert et al., 2007) as this would greatly affect the concentration of nutrients in terrestrial runoff.

The range of shear stress used in the erosion experiment (0.023 to 0.159 N m^{-2}) was within values observed to cause shallow water sediment resuspension (0.02 to 0.07 N m^{-2}) (Qin et al., 2004; Tang et al., 2020) and to naturally occur in spring tides and storms (0.11 to 0.28 N m^{-2}) (Kalnejais et al., 2007; Percuoco et al., 2015). Nevertheless, our shear stress values were lower than observed for wind dominated flow velocities in the Western Scheldt and Eastern Scheldt ($1.6 - 7 \text{ N m}^{-2}$) (de Vet et al., 2020).

The maximum sediment erosion depth of 6 mm obtained from our experiment (Appendix 6) was comparable to values from other studies (Kalnejais et al., 2010; Percuoco et al., 2015), and it was a higher than the daily bed level fluctuations observed in most locations (Appendix 9). However, it is noteworthy that a major storm event could erode between 2-3 cm (datasets mentioned in Hu et al., 2021) to as much as 20 cm of mudflat sediments (Yang et al., 2003; de Vet et al., 2020). This means that our experiment did not recreate a major storm event, but it caused greater erosion than observed from daily fluctuations. Notwithstanding, it is likely that our measurements underestimate the potential nutrient exchange that could occur

during a wind dominated erosion event in the Eastern Scheldt and WS because the imposed shear stress was lower than what could naturally occur in these systems (de Vet et al., 2020) and the maximum erosion depth was shallower than observed during major storm events (Hu et al., 2021). Despite this limitation, our results provide a first indication of differences in nutrient release between contrasting coastal systems and sites with different exposure.

To conclude, different nutrient exchange responses to sediment resuspension were detected in adjacent coastal systems with contrasting morphology, but also between sites with varied exposure to wave action. The magnitude of these exchanges generally increased with erosion speed and the duration of the disturbance. For instance, ammonium and nitrite release could be explained by erosion depth and pore water concentration. In contrast, phosphate release was much higher than predicted by erosion depth and porewater concentration at all estuarine sites, and it was even removed from the overlying water in the tidal bay stations. An erosion nutrient flux can be positive (i.e. additive) or negative (i.e. counterbalancing) compared to the undisturbed flux and comparable to several days of undisturbed fluxes. On this note, local characteristics of the site, such as exposure to wave action, were decisive for the magnitude of this effect with sheltered sites exhibiting a greater contribution in days of fluxes than exposed sites. We have demonstrated that sediment resuspension has the potential to alter the concentration of nutrients in the water column. This information could be used to assess whether algal blooms could occur following an intertidal sediments resuspension event.

Data availability statement

The raw data supporting the conclusions of this article will be made available by the authors, without undue reservation.

Author contributions

DR-Y did conceptualization, methodology, formal analysis, investigation, visualization, and wrote the original draft. TG did conceptualization, methodology, investigation, and revision of the draft. AD did investigation and revision of the draft. JT did conceptualization and revision of the draft. TB did conceptualization and revision of the draft. DO did conceptualization, supervision, and revision of the draft. KS did conceptualization, methodology, validation, formal analysis, supervision, and revision of the draft. All authors contributed to the article and approved the submitted version.

Funding

This research was supported by the project 'Coping with deltas in transition' within the Programme of Strategic Scientific Alliances between China and the Netherlands (PSA), financed by the Royal Netherlands Academy of Arts and Sciences (KNAW), Project No. PSA-SA-E-02.

Acknowledgments

We would like to thank the students Ivory Maast and Zono Heidemans for helping with the collection and processing of samples for this study. This work could not have been done without the help of the NIOZ analytical lab (Peter van Breugel, Yvonne Maas, Jan Peene, Jurian Brassers and more) which processed our sediment and water samples.

Conflict of interest

The authors declare that the research was conducted in the absence of any commercial or financial relationships that could be construed as a potential conflict of interest.

References

- Abril, G., Etcheber, H., le Hir, P., Bassoullet, P., Boutier, B., and Frankignoulle, M. (1999). Oxic/anoxic oscillations and organic carbon mineralization in an estuarine maximum turbidity zone (The Gironde, France). *Limnol Oceanogr* 44, 1304–1315. doi: 10.4319/lo.1999.44.5.1304
- Aller, R. C. (1982). *The effects of macrobenthos on chemical properties of marine sediment and overlying water*. In: McCall, P.L., Tevesz, M.J.S. (eds) *Animal-Sediment Relations*. Topics in Geobiology, vol 100. (Boston, MA: Springer) doi: 10.1007/978-1-4757-1317-6_2
- Amos, C. L., Brylinsky, M., Sutherland, T. F., O'Brien, D., Lee, S., and Cramp, A. (1998). The stability of a mudflat in the Humber estuary, south Yorkshire, UK. *Geological Society London Special Publications* 139, 25–43. doi: 10.1144/GSL.SP.1998.139.01.03
- Arndt, S., Regnier, P., and Vanderborgh, J.-P. (2009). Seasonally-resolved nutrient export fluxes and filtering capacities in a macrotidal estuary. *J. Mar. Syst.* 78, 42–58. doi: 10.1016/j.jmarsys.2009.02.008
- Baeyens, W., van Eck, B., Lambert, C., Wollast, R., and Goeyens, L. (1997). General description of the scheldt estuary. *Hydrobiologia* 366, 1–14. doi: 10.1023/a:1003164009031
- Bancon-Montigny, C., Gonzalez, C., Delpoux, S., Avenzac, M., Spinelli, S., Mhadhbi, T., et al. (2019). Seasonal changes of chemical contamination in coastal waters during sediment resuspension. *Chemosphere* 235, 651–661. doi: 10.1016/j.chemosphere.2019.06.213
- Borggaard, O. K. (1983). Effect of surface area and mineralogy of iron oxides on their surface charge and anion-adsorption properties. *Clays Clay Miner* 31, 230–232. doi: 10.1346/CCMN.1983.0310309
- Boynton, W. R., Ceballos, M. A. C., Bailey, E. M., Hodgkins, C. L. S., Humphrey, J. L., and Testa, J. M. (2018). Oxygen and nutrient exchanges at the sediment-water interface: A global synthesis and critique of estuarine and coastal data. *Estuaries Coasts* 41, 301–333. doi: 10.1007/s12237-017-0275-5
- Braeckman, U., Provoost, P., Gribsholt, B., van Gansbeke, D., Middelburg, J., Soetaert, K., et al. (2010). Role of macrofauna functional traits and density in biogeochemical fluxes and bioturbation. *Mar. Ecol. Prog. Ser.* 399, 173–186. doi: 10.3354/meps08336
- Breitburg, D., Levin, L. A., Oschlies, A., Grégoire, M., Chavez, F. P., Conley, D. J., et al. (2018). Declining oxygen in the global ocean and coastal waters. *Sci.* (1979) 359. doi: 10.1126/science.aam7240
- Cabrita, M. T., Catarino, F., and Vale, C. (1999). The effect of tidal range on the flushing of ammonium from intertidal sediments of the tagus estuary, Portugal. *Oceanologica Acta* 22, 291–302. doi: 10.1016/S0399-1784(99)80053-X
- Caraco, N., Cole, J., and Likens, G. (1990). A comparison of phosphorus immobilization in sediments of freshwater and coastal marine systems. *Biogeochemistry* 9, 277–290. doi: 10.1007/BF00000602
- Chen, N., Krom, M. D., Wu, Y., Yu, D., and Hong, H. (2018). Storm induced estuarine turbidity maxima and controls on nutrient fluxes across river-estuary-coast continuum. *Sci. Total Environ.* 628–629, 1108–1120. doi: 10.1016/j.scitotenv.2018.02.060
- Couceiro, F., Fones, G. R., Thompson, C. E. L., Statham, P. J., Sivy, D. B., Parker, R., et al. (2013). Impact of resuspension of cohesive sediments at the oyster grounds (North Sea) on nutrient exchange across the sediment–water interface. *Biogeochemistry* 113, 37–52. doi: 10.1007/s10533-012-9710-7
- De Borger, E., Tiano, J., Braeckman, U., Ysebaert, T., and Soetaert, K. (2020). Biological and biogeochemical methods for estimating bioirrigation: A case study in the oosterschelde estuary. *Biogeosciences* 17, 1701–1715. doi: 10.5194/bg-17-1701-2020
- de Vet, P. L. M., van Prooijen, B. C., Colosimo, I., Steiner, N., Ysebaert, T., Herman, P. M. J., et al. (2020). Variations in storm-induced bed level dynamics across intertidal flats. *Sci. Rep.* 10, 12877. doi: 10.1038/s41598-020-69444-7
- Dounas, C., Davies, I., Triantafyllou, G., Koulouri, P., Petihakis, G., Arvanitidis, C., et al. (2007). Large-Scale impacts of bottom trawling on shelf primary productivity. *Cont Shelf Res.* 27, 2198–2210. doi: 10.1016/j.csr.2007.05.006
- Dyer, K. R., Christie, M. C., Feates, N., Fennessy, M. J., Pejrup, M., and van der Lee, W. (2000). An investigation into processes influencing the morphodynamics of an intertidal mudflat, the dollard estuary, the Netherlands: I. hydrodynamics and suspended sediment. *Estuar. Coast. Shelf Sci.* 50, 607–625. doi: 10.1006/ecs.1999.0596
- Dzialowski, A. R., Wang, S. H., Lim, N. C., Beury, J. H., and Huggins, D. G. (2008). Effects of sediment resuspension on nutrient concentrations and algal biomass in reservoirs of the central plains. *Lake Reserv Manag* 24, 313–320. doi: 10.1080/07438140809354841
- Falcão, M., and Vale, C. (1995). Tidal flushing of ammonium from intertidal sediments of ria Formosa, Portugal. *Netherlands J. Aquat. Ecol.* 29, 239–244. doi: 10.1007/BF02084221
- Gilbert, A., Schaafsma, M., de Nocker, L., Liekens, I., and Broeckx, S. (2007). *Case study status report scheldt river basin*. (Netherlands: Flemish Institute for Technological Research (VITO) Belgium and Institute for Environmental Studies (IVM).
- Green, M. O., and Coco, G. (2014). Review of wave-driven sediment resuspension and transport in estuaries. *Rev. Geophysics* 52, 77–117. doi: 10.1002/2013RG000437
- Haan, C. T., Barfield, B. J., and Hayes, J. C. (1994). "Sediment properties and transport," in *Design hydrology and sedimentology for small catchments* (Elsevier), 204–237. doi: 10.1016/B978-0-08-057164-5.50011-6
- Herbert, R. (1999). Nitrogen cycling in coastal marine ecosystems. *FEMS Microbiol. Rev.* 23, 563–590. doi: 10.1016/S0168-6445(99)00022-4
- Hu, Z., Willemsen, P. W. J. M., Borsje, B. W., Wang, C., Wang, H., van der Wal, D., et al. (2021). Synchronized high-resolution bed-level change and biophysical data from 10 marsh–mudflat sites in northwestern Europe. *Earth Syst. Sci. Data* 13, 405–416. doi: 10.5194/essd-13-405-2021
- Jiang, L., Gerkema, T., Kromkamp, J. C., van der Wal, D., Carrasco de la Cruz, P. M., and Soetaert, K. (2020). Drivers of the spatial phytoplankton gradient in estuarine-coastal systems: Generic implications of a case study in a Dutch tidal bay. *Biogeosciences* 17, 4135–4152. doi: 10.5194/bg-17-4135-2020
- Jiang, L., Soetaert, K., and Gerkema, T. (2019). Decomposing the intra-annual variability of flushing characteristics in a tidal bay along the north Sea. *J. Sea Res.* 155, 101821. doi: 10.1016/j.seares.2019.101821
- Jodo, M., Kawamoto, K., Tochimoto, M., and Coverly, S. C. (1992). Determination of nutrients in seawater by segmented–flow analysis with higher analysis rate and reduced interference on ammonia. *J. Automatic Chem.* 14, 163–167. doi: 10.1155/S1463924692000300
- Jordan, T. E., Cornwell, J. C., Boynton, W. R., and Anderson, J. T. (2008). Changes in phosphorus biogeochemistry along an estuarine salinity gradient: The iron conveyor belt. *Limnol Oceanogr* 53, 172–184. doi: 10.4319/lo.2008.53.1.0172

Publisher's note

All claims expressed in this article are solely those of the authors and do not necessarily represent those of their affiliated organizations, or those of the publisher, the editors and the reviewers. Any product that may be evaluated in this article, or claim that may be made by its manufacturer, is not guaranteed or endorsed by the publisher.

Supplementary material

The Supplementary Material for this article can be found online at: <https://www.frontiersin.org/articles/10.3389/fmars.2023.1155386/full#supplementary-material>

- Kalnejais, L. H., Martin, W. R., and Bothner, M. H. (2010). The release of dissolved nutrients and metals from coastal sediments due to resuspension. *Mar. Chem.* 121, 224–235. doi: 10.1016/j.marchem.2010.05.002
- Kalnejais, L. H., Martin, W. R., Signell, R. P., and Bothner, M. H. (2007). Role of sediment resuspension in the remobilization of particulate-phase metals from coastal sediments. *Environ. Sci. Technol.* 41, 2282–2288. doi: 10.1021/es061770z
- Kornman, B. A., and Deckere, E. M. (1998). Temporal variation in sediment erodibility and suspended sediment dynamics in the dollard estuary. *Geological Society London Special Publications* 139, 231–241. doi: 10.1144/GSL.SP.1998.139.01.19
- Lessin, G., Artioli, Y., Almoth-Rosell, E., Blackford, J. C., Dale, A. W., Glud, R. N., et al. (2018). Modelling marine sediment biogeochemistry: Current knowledge gaps, challenges, and some methodological advice for advancement. *Front. Mar. Sci.* 5. doi: 10.3389/fmars.2018.00019
- Li, B., Cozzoli, F., Soissons, L. M., Bouma, T. J., and Chen, L. (2017). Effects of bioturbation on the erodibility of cohesive versus non-cohesive sediments along a current-velocity gradient: A case study on cockles. *J. Exp. Mar. Biol. Ecol.* 496, 84–90. doi: 10.1016/j.jembe.2017.08.002
- Loucaide, S., Cappelle, P. v., and Behrends, T. (2008). Dissolution of biogenic silica from land to ocean: Role of salinity and pH. *Limnol. Oceanogr.* 53, 1614–1621. doi: 10.4319/lo.2008.53.4.1614
- Malone, T. C., and Newton, A. (2020). The globalization of cultural eutrophication in the coastal ocean: Causes and consequences. *Front. Mar. Sci.* 7. doi: 10.3389/fmars.2020.00670
- Mestdagh, S., Fang, X., Soetaert, K., Ysebaert, T., Moens, T., and van Colen, C. (2020). Seasonal variability in ecosystem functioning across estuarine gradients: The role of sediment communities and ecosystem processes. *Mar. Environ. Res.* 162, 105096. doi: 10.1016/j.marenvres.2020.105096
- Middelburg, J. J., and Nieuwenhuize, J. (2000). Uptake of dissolved inorganic nitrogen in turbid, tidal estuaries. *Mar. Ecol. Prog. Ser.* 192, 79–88. doi: 10.3354/meps192079
- Morgan, B., Rate, A. W., and Burton, E. D. (2012). Water chemistry and nutrient release during the resuspension of FeS-rich sediments in a eutrophic estuarine system. *Sci. Total Environ.* 432, 47–56. doi: 10.1016/j.scitotenv.2012.05.065
- Morin, J., and Morse, J. W. (1999). Ammonium release from resuspended sediments in the Laguna madre estuary. *Mar. Chem.* 65, 97–110. doi: 10.1016/S0304-4203(99)00013-4
- Niemistö, J., Kononets, M., Ekeröth, N., Tallberg, P., Tengberg, A., and Hall, P. O. J. (2018). Benthic fluxes of oxygen and inorganic nutrients in the archipelago of gulf of Finland, Baltic Sea – effects of sediment resuspension measured in situ. *J. Sea Res.* 135, 95–106. doi: 10.1016/j.seares.2018.02.006
- Niemistö, J., and Lund-Hansen, L. C. (2019). Instantaneous effects of sediment resuspension on inorganic and organic benthic nutrient fluxes at a shallow water coastal site in the gulf of Finland, Baltic Sea. *Estuaries Coasts* 42, 2054–2071. doi: 10.1007/s12237-019-00648-5
- Nienhuis, P. H., and Smaal, A. C. (1994). “The oosterschelde estuary, a case-study of a changing ecosystem: An introduction,” in *The oosterschelde estuary (The Netherlands): A case-study of a changing ecosystem* (Dordrecht: Springer Netherlands), 1–14. doi: 10.1007/978-94-011-1174-4_1
- Ogilvie, B. G., and Mitchell, S. F. (1998). Does sediment resuspension have persistent effects on phytoplankton? experimental studies in three shallow lakes. *Freshw. Biol.* 40, 51–63. doi: 10.1046/j.1365-2427.1998.00331.x
- Paterson, D. M., Hope, J. A., Kenworthy, J., Biles, C. L., and Gerbersdorf, S. U. (2018). Form, function and physics: The ecology of biogenic stabilisation. *J. Soils Sediments* 18, 3044–3054. doi: 10.1007/s11368-018-2005-4
- Percuoco, V. P., Kalnejais, L. H., and Officer, L. V. (2015). Nutrient release from the sediments of the great bay estuary, N.H. USA. *Estuar. Coast. Shelf Sci.* 161, 76–87. doi: 10.1016/j.ecss.2015.04.006
- Precht, E., Franke, U., Polerecky, L., and Huettel, M. (2004). Oxygen dynamics in permeable sediments with wave-driven pore water exchange. *Limnol. Oceanogr.* 49, 693–705. doi: 10.4319/lo.2004.49.3.0693
- QGIS Development Team (2021). QGIS geographic information system. Open Source Geospatial Foundation Project. Available at: <http://qgis.osgeo.org>
- Qin, B., Hu, W., Gao, G., Luo, L., and Zhang, J. (2004). Dynamics of sediment resuspension and the conceptual schema of nutrient release in the large shallow lake taihu, China. *Chin. Sci. Bull.* 49, 54. doi: 10.1360/03wd0174
- R Core Team (2020). *R: A language and environment for statistical computing*. (Vienna, Austria: R Foundation for Statistical Computing). Available at: <https://www.R-project.org/>
- Rios-Yunes, D., Tiano, J. C., van Oevelen, D., van Dalen, J., and Soetaert, K. (2023a). Annual biogeochemical cycling in intertidal sediments of a restored estuary reveals dependence of n, p, c and Si cycling to temperature and water column properties. *Estuar. Coast. Shelf Sci.* 108227. doi: 10.1016/j.ecss.2023.108227
- Rios-Yunes, D., Tiano, J. C., van Rijswijk, P., de Borger, E., van Oevelen, D., and Soetaert, K. (2023b). Long-term changes in ecosystem functioning of a coastal bay expected from a shifting balance between intertidal and subtidal habitats. *Cont. Shelf Res.* 254. doi: 10.1016/j.csr.2022.104904
- Schallenberg, M., and Burns, C. W. (2004). Effects of sediment resuspension on phytoplankton production: teasing apart the influences of light, nutrients and algal entrainment. *Freshw. Biol.* 49, 143–159. doi: 10.1046/j.1365-2426.2003.01172.x
- Shaughnessy, A. R., Sloan, J. J., Corcoran, M. J., and Hasenmueller, E. A. (2019). Sediments in agricultural reservoirs act as sinks and sources for nutrients over various timescales. *Water Resour. Res.* 55, 5985–6000. doi: 10.1029/2018WR024004
- Shrestha, P. L., Kaluarachchi, I. D., Anid, P. J., Blumberg, A. F., and DiToro, D. M. (2001). “Cohesive sediment resuspension: Experimentation and analysis,” in *Bridging the gap* (Reston, VA: American Society of Civil Engineers), 1–8. doi: 10.1061/40569(2001)258
- Slomp, C. P., Epping, E. H. G., Helder, W., and Raaphorst, W. (1996). A key role for iron-bound phosphorus in authigenic apatite formation in north Atlantic continental platform sediments. *J. Mar. Res.* 54, 1179–1205. doi: 10.1357/0022240963213745
- Smaal, A. C., and Nienhuis, P. H. (1992). The eastern scheldt (The Netherlands), from an estuary to a tidal bay: A review of responses at the ecosystem level. *Netherlands J. Sea Res.* 30, 161–173. doi: 10.1016/0077-7579(92)90055-J
- Soetaert, K., Middelburg, J. J., Heip, C., Meire, P., van Damme, S., and Maris, T. (2006). “Long-term change in dissolved inorganic nutrients in the heterotrophic scheldt estuary,” in *Limnology and oceanography* (Belgium, The Netherlands: American Society of Limnology and Oceanography Inc), 409–423. doi: 10.4319/lo.2006.51.1_part_2.0409
- Soetaert, K., Vincx, M., Wittoeck, J., Tulkens, M., and Van Gansbeke, D. (1994). Spatial patterns of westerschelde meiobenthos. *Estuar. Coast. Shelf Sci.* 39, 367–388. doi: 10.1006/ecss.1994.1070
- Statham, P. J. (2012). Nutrients in estuaries - an overview and the potential impacts of climate change. *Sci. Total Environ.* 434, 213–227. doi: 10.1016/j.scitotenv.2011.09.088
- Struyf, E., van Damme, S., Gribsholt, B., Middelburg, J., and Meire, P. (2005). Biogenic silica in tidal freshwater marsh sediments and vegetation (Schelde estuary, Belgium). *Mar. Ecol. Prog. Ser.* 303, 51–60. doi: 10.3354/meps303051
- Struyf, E., Van Damme, S., and Meire, P. (2004). Possible effects of climate change on estuarine nutrient fluxes: A case study in the highly nutrient rich schelde estuary (Belgium, the Netherlands). *Estuar. Coast. Shelf Sci.* 60, 649–661. doi: 10.1016/j.ecss.2004.03.004
- Tang, C., Li, Y., He, C., and Acharya, K. (2020). Dynamic behavior of sediment resuspension and nutrients release in the shallow and wind-exposed meiliang bay of lake taihu. *Sci. Total Environ.* 708. doi: 10.1016/j.scitotenv.2019.135131
- ten Brinke, W. B. M. (1994). “Hydrodynamic and geomorphological changes in the tidal system,” in *The oosterschelde estuary (The Netherlands): a case-study of a changing ecosystem* (Dordrecht: Springer Netherlands), 15–16. doi: 10.1007/978-94-011-1174-4_2
- Tengberg, A., Almroth, E., and Hall, P. (2003). Resuspension and its effects on organic carbon recycling and nutrient exchange in coastal sediments: *In situ* measurements using new experimental technology. *J. Exp. Mar. Biol. Ecol.* 285–286, 119–142. doi: 10.1016/S0022-0981(02)00523-3
- Tiano, J. C., de Borger, E., O’Flynn, S., Cheng, C. H., van Oevelen, D., and Soetaert, K. (2021). Physical and electrical disturbance experiments uncover potential bottom fishing impacts on benthic ecosystem functioning. *J. Exp. Mar. Biol. Ecol.* 545, 151628. doi: 10.1016/j.jembe.2021.151628
- Tiano, J. C., Witbaard, R., Bergman, M. J. N., van Rijswijk, P., Tramper, A., van Oevelen, D., et al. (2019). Acute impacts of bottom trawl gears on benthic metabolism and nutrient cycling. *ICES J. Mar. Sci.* 76, 1917–1930. doi: 10.1093/icesjms/fsz060
- Turner Designs (n.d.) *S-0243 Cyclops-7 or 7F calibration using liquid dye standards* (Accessed February 28, 2023).
- Wetsteyn, L. P. M. J., and Kromkamp, J. C. (1994). Turbidity, nutrients and phytoplankton primary production in the oosterschelde (The Netherlands) before, during and after a large-scale coastal engineering project, (1980–1990). *Hydrobiologia* 282–283, 61–78. doi: 10.1007/BF00024622
- Widdows, J., Brinsley, M., Salkeld, P., and Lucas, C. (2000a). Influence of biota on spatial and temporal variation in sediment erodibility and material flux on a tidal flat (Westerschelde, the Netherlands). *Mar. Ecol. Prog. Ser.* 194, 23–37. doi: 10.3354/meps194023
- Widdows, J., Brown, S., Brinsley, M. D., Salkeld, P. N., and Elliott, M. (2000b). Temporal changes in intertidal sediment erodibility: Influence of biological and climatic factors. *Cont. Shelf Res.* 20, 1275–1289. doi: 10.1016/S0278-4343(00)00023-6
- Woth, K., Weisse, R., and von Storch, H. (2006). Climate change and North Sea storm surge extremes: An ensemble study of storm surge extremes expected in a changed climate projected by four different regional climate models. *Ocean Dyn.* 56, 3–15. doi: 10.1007/s10236-005-0024-3
- Yang, S.-L., Friedrichs, C. T., Shi, Z., Ding, P.-X., Zhu, J., and Zhao, Q.-Y. (2003). Morphological response of tidal marshes, flats and channels of the outer Yangtze river mouth to a major storm. *Estuaries* 26, 1416–1425. doi: 10.1007/BF02803650
- Ysebaert, T., Meire, P., Maes, D., and Buijs, J. (1993). The benthic macrofauna along the estuarine gradient of the schelde estuary. *Netherlands J. Aquat. Ecol.* 27, 327–341. doi: 10.1007/BF02334796
- Ysebaert, T., van der Hoek, D. J., Wortelboer, R., Wijsman, J. W., Tangelde, M., and Nolte, A. (2016). Management options for restoring estuarine dynamics and implications for ecosystems: A quantitative approach for the Southwest Delta in the Netherlands. *Ocean & Coastal Management* 121, 33–48. doi: 10.1016/j.ocecoaman.2015.11.005